Quantum billiards in a rotating boundary

1989 J. Phys. A: Math. Gen. 22 3537

(http://iopscience.iop.org/0305-4470/22/17/019)

J. Phys. A: Math. Gen. **22** (1989) 3537-3550. Printed in the UK

Quantum billiards in a rotating boundary

D K Siegwart

Department of Mathematical Sciences, Science Laboratories, University of Durham, South Road, Durham, UK

Received 22 December 1988, in final form 24 April 1989

Abstract. An example of billiards in a moving boundary, which exhibits regular and chaotic motion, has been discovered recently. The specific system is the motion of a particle inside a circular billiard table which rotates uniformly about a point on its edge. At one energy the motion becomes ergodic, but is regular for very low and for very high energies.

In the present work we study the quantum mechanics of the system, and calculate numerically the energy spectrum. In the semiclassical limit, we show that for energies near to where the system is ergodic, the level spacing distribution is Wigner. As $\hbar \to \infty$ the system becomes equivalent to the stationary case, but the spectral statistics for low energies is indistinguishable between Wigner and Poissonian. For some intermediate $\hbar$ we find that the distribution becomes very Poissonian even though the energy levels used are in the chaotic region of the classical motion.

1. Introduction

Little work has been done on billiard systems which exhibit chaos purely due to the rotation of the boundary. Most work has been carried out on systems where chaotic motion is due to the shape of the boundary, such as the stadium of Bunimovich [1], the Sinai billiards [2], heart-shaped boundaries [3], or due to magnetic fields such as the elliptical billiards of Berry and Robnik [4] and the Aharonov-Bohm billiards [5]. Rotation is one of the simplest ways of introducing chaos to regular motion. We consider the simplest such system, a circular billiard rotating in its own plane about a point on its edge. This has the interesting property that for no rotation the system is simply a circular billiard, which is of course fully separable, and thus a superb example of regular motion. But as soon as rotation is introduced the system has regions of phase space which are very chaotic. For a particular energy hypersurface, the proportion of phase space which is chaotic depends on the energy. For low and high energies it is small, but for intermediate values it is quite high, peaking at critical energy where no regular regions can be seen, and this happened close to a bifurcation of a fixed point into a two-cycle. These were facts gathered in a previous paper, Fairlie and Siegwart [6]. The purpose of this paper is to study the quantum mechanics of this system.

The correspondence principle has been used widely in quantum mechanics to predict properties of quantum systems from their classical analogues. Torus quantisation is one such example where the conservation of quantities other than energy in the classical system implies the quantisation of those quantities in the quantum system, and adds extra labels to the energy eigenvalue. However, for classically chaotic systems such quantities are no longer conserved. For example, a circular billiard has conserved

0305-4470/89/173537+14$02.50

angular momentum about the centre, but the stadium of Bunimovich has not. Then torus quantisation is impossible, and the quantum system has very different properties. The wavefunction cannot be properly labelled, and so there is a loss of information about the state. Not only does the wavefunction give a probabilistic description of physical laws, but it is itself statistical in nature. Much work has been done by Dyson, Mehta, Porter and others [7] using these ideas for the energy levels of nuclei. Because these properties are fundamentally different from the usual quantum properties it seems justified to call them examples of 'quantum chaos', although a proper definition of this term has not been made.

It is not at all easy to formulate a mathematical framework for such systems, and it becomes necessary to study a wide variety of particular examples, in order to find some common properties, which can then be tied to a proper mathematical foundation. Present work centres on numerical analysis, and the use of present theories in regimes where maybe they are strained.

In this paper we continue this approach in the hope that we can gain some insight into quantum chaos. In particular, we look at energy level statistics, and test predictions about the energy level spacings distribution $P(S)$, where S is the ratio of the nearest-neighbour spacing to the local mean spacing. Classically integrable systems have been shown by Berry and Tabor to have Poissonian statistics [8]:

$$P(S) \approx e^{-S}. \tag{1}$$

But time-reversible ergodic systems are expected to have Gaussian orthogonal ensemble (GOE) statistics [9]:

$$P(S) \approx (\pi/2)S \exp(-\pi S^2/4). \tag{1.2}$$

Time-violating ergodic systems are expected to have Gaussian unitary ensemble (GUE) statistics [10]:

$$P(S) \approx (32S^2/\pi^2) \exp(-4S^2/\pi). \tag{1.3}$$

Energy levels of classically chaotic systems are eigenvalues of infinite-dimensional matrices, which are expected to behave as typical members of random matrix ensembles. If the Hamiltonian has time-reversal symmetry (T), then the ensemble consists of real symmetric matrices (GOE) and obeys (1.2). If the Hamiltonian does not have T, nor an equivalent symmetry, then the ensemble consists of complex Hermitian matrices (GUE) and obeys (1.3).

Our system does not have T, but the Hamiltonian is invariant under S_xT, time reversal with reflection in the x axis. This is the 'false' time-reversal symmetry of Robnik and Berry, and so it is expected to be GOE-like.

2. The Hamiltonian

We use the same terminology as [6]. A free particle of unit mass is inside a circular billiard table of unit radius, rotating at unit angular velocity about a point on its edge, which is chosen to be the origin. We transform to the rotating frame in which the boundary is stationary, and obtain the classical Hamiltonian

$$H = p_x^2 + p_y^2 - 2(xp_y - yp_x) \tag{2.1}$$

where (x, y) is the position of the particle in the rotating frame, and (p_x, p_y) is its conjugate momentum. We then replace $\boldsymbol{p}$ by the operator $-i\hbar\nabla$ such that

$$H = -\hbar^2\nabla^2 + 2i\hbar\partial_\theta. \tag{2.2}$$

We look at the rescaled Hamiltonian

$$\mathscr{H} = -\nabla^2 + 2i\alpha\partial_\theta \tag{2.3}$$

where $\alpha = 1/\hbar$. This can also be written

$$\mathscr{H} = -(\partial_i - i\alpha\varepsilon_{ij}x_j)^2 - \alpha^2 x_i^2 \tag{2.4}$$

which shows that the system is equivalent to a particle in a uniform magnetic field of strength 2 ($A_i = \varepsilon_{ij}x_j$) and in a quadratic potential field $V = -x_i^2$.

Wavefunctions are made up of superpositions of eigenstates $\psi(\boldsymbol{x})\exp(-i\mathscr{E}t)$. The ψ must satisfy the stationary Schrödinger equation $\mathscr{H}\psi = \mathscr{E}\psi$. The solution of this eigenvalue problem is made very tricky by the condition that $\psi = 0$ on the boundary. This does not suit the form of (2.3), so we transform coordinates to the centre of the circle. The nice ∂_θ is transformed to something less agreeable. In polar coordinates we get for the Schrödinger equation

$$\mathscr{H}\psi = -\nabla^2\psi + 2i\alpha\left[\left(1 + \frac{\cos\theta}{r}\right)\frac{\partial}{\partial\theta} + \sin\theta\frac{\partial}{\partial r}\right]\psi = \mathscr{E}\psi. \tag{2.5}$$

Now choosing the orthonormal basis functions

$$\phi_{ml} = N_{ml}J_m(\lambda_{ml}r)\exp(im\theta) \tag{2.6}$$

where λ_{ml} are the zeros of the Bessel functions, and

$$N_{ml} = [\sqrt{\pi}J'_m(\lambda_{ml})]^{-1} \tag{2.7}$$

we obtain the matrix elements of $\mathscr{H}$

$$\mathscr{H}_{mlnk} = \langle nk|\mathscr{H}|ml\rangle$$
$$= \begin{cases} \lambda_{ml}^2 - 2\alpha m & \text{for } k = l,\ n = m \\ -2\pi\alpha\lambda_{ml}N_{ml}N_{nk}\displaystyle\int_0^1 dr\, rJ_m(\lambda_{ml}r)J_n(\lambda_{nk}r) & \text{for } n = m \pm 1 \\ 0 & \text{elsewhere.} \end{cases} \tag{2.8}$$

The Bessel functions were computed to 14-figure accuracy using NAG routines for $J_0(x)$ and $J_1(x)$ and calculating $J_n(x)$ from these by upward recursion for large x $(x > n)$, and downward recursion for small x. The zeros were found by bracketing the root using McMahon's formula and the asymptotic formula for large orders [11] then using Newton-Raphson and bisection methods, and were sorted in ascending order. The integrations were computed to ten figures using an adaptive Gauss 30-point and Kronrod 61-point NAG routine. This is particularly good for oscillating integrands. Diagonalisation was performed using another NAG routine which reduces matrices to real symmetric tridiagonal form, and then uses the QL algorithm. Press *et al* [12] was a very useful source for many of these routines.

The eigenvalues are the diagonal elements of the diagonalised Hamiltonian matrix. When $\alpha = 0$ the matrix is already diagonal; the basis functions are also eigenfunctions. But the diagonal elements λ_{ml}^2 are not in ascending order. We expect the high-lying

levels to be most affected as α increases, so the matrix was re-ordered so that the low-lying levels are the first to be calculated. This will increase the reliability of the computed eigenvalues. We thus sort the zeros λ_{ml} in ascending order, using the mapping obtained $[m, l] \mapsto i$ to re-order the Hamiltonian matrix

$$\mathcal{H}_{ij} = \mathcal{H}_{m(i)l(i)n(j)k(j)}. \tag{2.9}$$

In order to diagonalise this matrix numerically we need to truncate it to a finite size. The difficulty is knowing when the truncated matrix is a good approximation for the infinite one. Resorting the matrix elements as above must help, because we expect that the eigenvalues for $\alpha \neq 0$ are similar to those at $\alpha = 0$, at least for small α. But as $\alpha \to \infty$ (the semiclassical limit $\hbar \to 0$) high-lying elements of the matrix are likely to affect the low-lying elements significantly. It is hard to tell whether the limiting matrix is even diagonalisable. Presumably it is, because otherwise a semiclassical limit would not be possible. My own solution to this problem was to always diagonalise two matrices of different size (in this case 300×300 and 380×380) and to then compare their eigenvalues. If the relative error of eigenvalues is greater than 10%, that value is rejected. By this criterion it was possible to diagonalise matrices in the range $0 \leqslant \alpha \leqslant 15$. 75 matrices of each size were diagonalised within this range. Only the first 60 gave enough accurate eigenvalues to be used.

Later we will wish to compare the eigenvalues $\mathcal{E}_i$ to the classical energy. In [6] we used the kinetic energy K of the particle at the point furthest from the pivot to define the energy hypersurface. The corresponding quantised energy levels K_i are given by

$$K_i(\alpha) = \mathcal{E}_i(\alpha)/2\alpha^2 + 2. \tag{2.10}$$

When $K = 2$ the classical phase space has no recognisable structure, and about 98% of its volume is chaotic. The limits $K \to 0$ and $K \to \infty$ give integrable systems. So we expect eigenvalues K_i centred on $K = 2$ to be the most chaotic.

3. The energy levels

The lowest 50 eigenvalues $\mathcal{E}_i(\alpha)$ of each matrix are plotted against the parameter α in figure 1. For small α and high energy there are a large number of apparent crossings, but the resolution of the graph is not good enough to distinguish whether these are real or not. Upon closer inspection some appear to be real, but they are more likely to be avoided crossings with exceedingly narrow separations of the order $\exp(-\text{constant}/\hbar)$. This is predicted by Berry [13] for integrable systems from consideration of tunnelling between neighbouring tori (which is disregarded in the semiclassical torus quantisation). Thus much of the spectrum for low α appears to be 'regular'. However, for large α and low energies the pattern of the spectrum changes. There are fewer level crossings, and those which do exist are actually avoided crossings. The energy levels are also much more evenly distributed. This is the transition of the regular spectrum where there is a large probability of near degeneracies ($P(S) \to$ constant as $S \to 0$) to a chaotic spectrum where there is level repulsion and hence little probability of degeneracies ($P(S) \to 0$ as $S \to 0$). Each near crossing shows strong mixing between states, and wavefunctions appear to exchange quantum numbers. This is manifested by the exchange of their slopes $\mathrm{d}\mathcal{E}_i/\mathrm{d}\alpha$. Such mixing is required many times if we expect regular (in fact separable) energy levels at $\alpha = 0$ to be continuously deformed

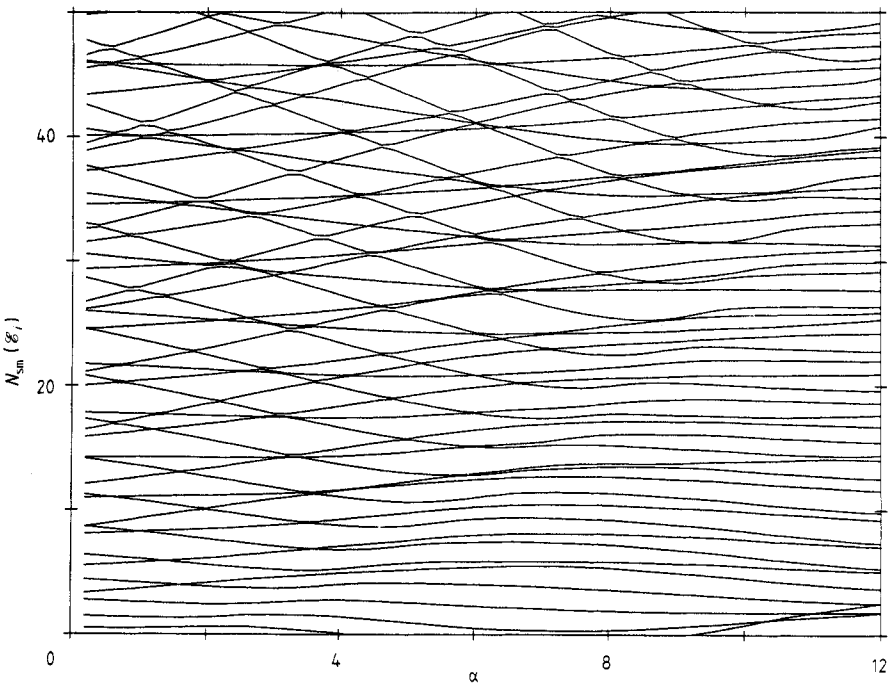

Figure 1. The unfolded energy-level spectrum $N_{sm}(\mathscr{E}_i)$ for the rotating circle parametrised by $\alpha = 1/\hbar$.

to the 'random' energy levels in the chaotic region. For regular wavefunctions the energy levels are purely determined by their quantum numbers, so there is no correlation between them. So the energy spacing distribution is Poissonian. However for chaotic wavefunctions an energy level is not purely determined by its quantum numbers because its quantum numbers are not sufficient to label the state, so there must be correlation between it and other energy levels. This implies that $P(S)$ is not Poissonian.

The energy level spacing distribution is not a very useful property to plot directly. $P(S)$ can only be computed averaged over an interval, and in order to have enough eigenvalues in each interval (or bin) a large size of bin is required, which reduces the resolution of the graph. It is more natural to use the integral distribution:

$$I(S) = \int_0^S P(x)\,\mathrm{d}x = \lim_{N\to\infty} \frac{1}{N} \sum_{i=1}^{N} \Theta(S - S_i) \tag{3.1}$$

and then the spacing values are used fully. $I(S)$ is approximated by the empirical distribution function (EDF)

$$I_N(S) = \frac{1}{N} \sum_{i=1}^{N} \Theta(S - S_i) \tag{3.2}$$

where S_i is the ratio of the ith level spacing to the local mean level spacing, $\overline{\Delta\mathscr{E}}(\mathscr{E})$. $\overline{\Delta\mathscr{E}}(\mathscr{E})$ is determined from the gradient of the smoothed spectral staircase, $N_{sm}(\mathscr{E})$, which is approximated by fitting a sufficiently smooth curve to the spectral staircase, $N(\mathscr{E}) = \Sigma_{i=1}^{\infty} \Theta(\mathscr{E} - \mathscr{E}_i)$. The semiclassical Weyl rule with corrections, for a stationary boundary gives a fitting form which has terms in $\mathscr{E}$ and $\sqrt{\mathscr{E}}$. The rotation causes

deviation from this rule, and a good fit was obtained only when a quadratic term was added:

$$N_{\mathrm{sm}}(\mathscr{E}) = a + b\mathscr{E} + c\sqrt{\mathscr{E}} + d\mathscr{E}^2 \tag{3.3}$$

where a, b, c, d are constants. So

$$\overline{\Delta\mathscr{E}}(\mathscr{E}) = \left(\frac{\mathrm{d}N_{\mathrm{sm}}}{\mathrm{d}\mathscr{E}}(\mathscr{E})\right)^{-1}. \tag{3.4}$$

We would like to investigate the spectrum around a particular energy K to see whether its statistics are related to the degree of chaos in the classical phase space. Thus $I_N(S)$ was computed for several ranges of the quantum label i of the energy level K_i. There are two properties we wish to maximise: we wish there to be a large number of eigenvalues in order to distinguish between different statistics, but opposing this we wish the energy range to be small enough in order that the classical phase space does not change significantly over the energy range. To be able to do this well we require $\hbar$ to be small (α large). Ranges $i = 1$ to 50, $i = 50$ to 100, $i = 100$ to 150 were chosen. The energy ranges to which these correspond are shown in table 1. The combined ranges $i = 1$ to 100 and $i = 1$ to 150 were also used. To each distribution the Kolmogorov-Smirnov and the W^2 EDF statistics tests were applied [14], to determine the goodness of fit to either a Poisson or a GOE distribution. The W^2 test is the most powerful because it uses all the data points to evaluate the statistic, whereas the Kolmogorov-Smirnov test uses only one. The results for the W^2 test are shown in table 2. Let us consider the lowest 50 eigenvalues. For low α the test accepts both distributions, so we cannot say which distribution the data fits. For α in the range 3.2-3.8 and 5.8-6.6 the data fits only the Poisson, and for α in the range 4.0-5.4 and 6.8-12.0 the data fits only the GOE. Above $\alpha = 12.0$ the energy levels lose accuracy. The results show that the spectrum does behave as expected for large α. However there is not a smooth transition from Poisson to GOE statistics as we might have expected, but an intermittent one. At one point the spectrum becomes extremely regular, where we might have expected it to be quite chaotic. We have no explanation for why this happens. The next range of eigenvalues from $i = 50$-100 has an energy range which does not enter the chaotic region until α is about 8 or 9. There is some evidence for a transition in the spectrum near $\alpha = 8.8$, but above this eigenvalues are unreliable, and there is again evidence for GOE statistics for small α (near 3.8). The spectrum for $i = 100$-150 shows little evidence for GOE statistics in the range of $\alpha = 0.0$-5.0 which could be tested. This is expected, because none of the energies enter the chaotic region. For $i = 1$-100 and $i = 1$-150 the larger number of eigenvalues will make the statistical tests more powerful, but the energy range is too large to expect uniform statistics except at very low α, where we expect Poissonian statistics almost everywhere. Typical members of these sets of distributions are shown in figure 2. Although sometimes it is not possible to reliably distinguish between pure statistics, and statistics which are a mixture of Poisson and GOE, many of the EDF are much closer to one of the theoretical distributions than would be expected by statistical analysis. Such effects have been mentioned before, for example in [5]. Because of these effects, this method of fitting the EDF to a model distribution was tried, even though the statistics may not be powerful enough for 50 values to justify the significance of the fit. It is assumed as an approximation that there are two types of energy levels, one Poissonian and the other GOE, whose mixture is constant over the energy range

Table 1. The first, 50th, 100th and 150th energy eigenvalues of the rotating circle as defined by the equation for K_i in the text. It shows that the energy range condenses onto the most chaotic strata for energy hypersurface in phase space. Note that the energy is parametrised by $\alpha = 1/\hbar$.

α	$\hbar$	K_1	K_{50}	K_{100}	K_{150}
0.400	2.5000	19.8	1276.9	2549.9	3810.3
0.800	1.2500	6.2	316.6	627.2	940.6
1.200	0.8333	3.7	139.9	274.3	413.0
1.600	0.6250	2.7	78.3	152.4	231.5
2.000	0.5000	2.2	49.1	97.3	147.1
2.400	0.4167	1.9	34.0	67.6	101.8
2.800	0.3571	1.7	24.8	49.7	74.3
3.200	0.3125	1.5	19.0	38.1	57.0
3.600	0.2778	1.4	15.2	30.2	44.8
4.000	0.2500	1.3	12.5	24.5	36.4
4.400	0.2273	1.2	10.3	20.1	30.1
4.800	0.2083	1.1	8.6	16.8	25.1
5.200	0.1923	1.1	7.4	14.3	21.4
5.600	0.1786	1.0	6.5	12.3	18.5
6.000	0.1667	1.0	5.9	10.8	16.2
6.400	0.1563	0.9	5.3	9.5	14.2
6.800	0.1471	0.9	4.7	8.5	12.6
7.200	0.1389	0.8	4.3	7.7	11.3
7.600	0.1316	0.8	4.0	6.9	10.2
8.000	0.1250	0.8	3.7	6.4	9.3
8.400	0.1190	0.8	3.4	5.9	8.4
8.800	0.1136	0.7	3.2	5.4	7.7
9.200	0.1087	0.7	3.0	5.0	7.1
9.600	0.1042	0.7	2.8	4.7	6.5
10.000	0.1000	0.7	2.7	4.4	6.1
10.400	0.0962	0.7	2.5	4.2	5.7
10.800	0.0926	0.6	2.4	3.9	5.4
11.200	0.0893	0.6	2.3	3.6	5.0
11.600	0.0862	0.6	2.2	3.4	4.8
12.000	0.0833	0.6	2.2	3.3	4.5

considered. The resulting distribution depends on one parameter, the proportions of each type. The integral distribution is

$$I(S;\mu) = 1 - \mu \exp(-\nu x) \exp[-\tfrac{1}{4}\pi(\mu x)^2] - \nu \exp(-\nu x) \operatorname{erfc}(\tfrac{1}{2}\sqrt{\pi}\mu x) \tag{3.5}$$

where μ is the proportion of GOE eigenvalues and ν that of Poissonian eigenvalues, so $\mu + \nu = 1$. Berry and Robnik [15] have calculated the semiclassical distribution when the energy levels are chosen in a narrow interval. This depends on the Liouville measure of the sum of the classically regular regions and on the separate Liouville measures of the large chaotic regions. If there is more than one large chaotic region, then the distribution is not of the form of (3.5) *in the semiclassical limit.* However, it is the transition region for which we are using (3.5) and here there is no theoretical result, because the system is not semiclassical and the energy interval is large. The data were fitted to the integral distribution rather than to $P(S;\mu)$ because more detail is included in $I(S;\mu)$. The resulting fitting parameter μ for the three ranges of energy levels is plotted against α in figure 3. Clearly there is a sharp change in statistics at $\alpha = 6$ for the lowest 50 eigenvalues. This is reflected in similar transitions for the higher

Table 2. The W^2 statistic $W^2_{n_1,n_2}$ for the n_1^{th} eigenvalue to the n_2^{th} eigenvalue. Table 1 gives the corresponding energy ranges. The rejection of the fit is at a significance level of 5% (critical $W^2_{cr} = 0.460$). The A or R after the statistic denotes acceptance or rejection respectively of the fit.

	W^2 statistic for Wigner distribution			W^2 statistic for Poisson distribution		
α	$W^2_{1,50}$	$W^2_{50,100}$	$W^2_{100,150}$	$W^2_{1,50}$	$W^2_{50,100}$	$W^2_{100,150}$
0.4	0.300 A	0.604 R	0.507 R	0.257 A	0.124 A	0.101 A
0.8	0.257 A	0.441 A	0.546 R	0.294 A	0.162 A	0.074 A
1.2	0.228 A	0.578 R	0.576 R	0.400 A	0.081 A	0.084 A
1.6	0.267 A	0.770 R	0.785 R	0.416 A	0.063 A	0.066 A
2.0	0.320 A	0.624 R	0.390 A	0.235 A	0.045 A	0.144 A
2.4	0.166 A	0.552 R	0.272 A	0.328 A	0.140 A	0.232 A
2.8	0.300 A	0.392 A	0.703 R	0.293 A	0.176 A	0.135 A
3.2	0.523 R	0.284 A	1.068 R	0.100 A	0.338 A	0.040 A
3.6	0.478 R	0.279 A	0.941 R	0.161 A	0.299 A	0.043 A
4.0	0.219 A	0.333 A	1.003 R	0.508 R	0.179 A	0.035 A
4.4	0.237 A	0.479 R	0.972 R	0.482 R	0.112 A	0.087 A
4.8	0.185 A	0.912 R	1.277 R	0.822 R	0.043 A	0.048 A
5.2	0.131 A	1.854 R	0.742 R	0.695 R	0.174 A	0.051 A
5.6	0.302 A	1.413 R	0.638 R	0.229 A	0.056 A	0.056 A
6.0	0.852 R	1.086 R	0.780 R	0.113 A	0.039 A	0.041 A
6.4	0.809 R	0.857 R	1.317 R	0.115 A	0.073 A	0.051 A
6.8	0.179 A	0.656 R	1.086 R	0.500 R	0.058 A	0.062 A
7.2	0.270 A	0.701 R	0.903 R	0.630 R	0.062 A	0.353 A
7.6	0.113 A	0.812 R	1.025 R	1.236 R	0.026 A	0.066 A
8.0	0.071 A	0.646 R	1.254 R	0.659 R	0.065 A	0.136 A
8.4	0.055 A	0.533 R	2.038 R	0.894 R	0.150 A	0.281 A
8.8	0.071 A	0.317 A	1.850 R	0.826 R	0.247 A	0.310 A
9.2	0.112 A	0.695 R	1.846 R	0.685 R	0.058 A	0.345 A
9.6	0.074 A	0.739 R	3.115 R	0.968 R	0.114 A	0.671 R
10.0	0.097 A	0.958 R	3.906 R	1.182 R	0.102 A	0.940 R
10.4	0.080 A	1.353 R	3.904 R	1.026 R	0.078 A	0.927 R
10.8	0.128 A	0.764 R	1.867 R	1.232 R	0.028 A	0.362 A
11.2	0.129 A	0.503 R	1.027 R	1.509 R	0.202 A	0.147 A
11.6	0.159 A	0.178 A	0.782 R	1.836 R	0.609 R	0.196 A
12.0	0.196 A	0.138 A	1.455 R	2.281 R	0.436 A	0.161 A

levels. The lower eigenvalues also seem to fit a purely GOE distribution for α above 9.6. This tails off after $\alpha = 11.4$, but this may to be due to loss of accuracy in the eigenvalues. From the randomness of the data and the empirical form of (3.5), we do not expect to form any other conclusions from this fit.

4. Lyapunov exponents and chaotic volume

Using the standard method of Bennettin and Strelcyn [16], we calculate the Lyapunov exponent $\Lambda(x)$ of a trajectory $x(t)$ in phase space. $\Lambda(x)$ is a limiting value calculated over a large number of reflections. We have found numerically that Λ is independent of the length and direction of the initial separation vector δx, but that small fluctuations in Λ are observed (of approximately 3%) as it approaches its limiting value even after 10 000 reflections. This is in agreement with the work of Bennettin and Strelcyn.

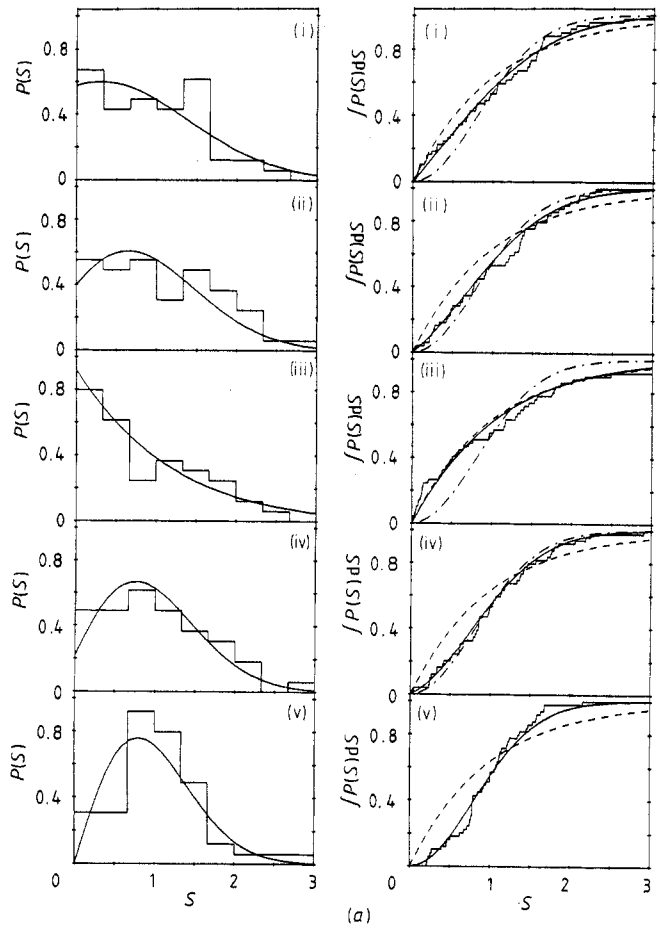

Figure 2. The level spacing distribution (left) and the integral (cumulative) distribution (right) for the rotating circle. The broken curve is the Poisson distribution, the chain curve is the Wigner distribution and the full curve is the distribution found by fitting the data by least squares to equation (3.5). The figures (i)-(v) correspond to $\alpha = 2, 4, 6, 8, 10$ respectively, and are drawn for (*a*) the first 50 eigenvalues (*b*) the next 50 eigenvalues (*c*) the eigenvalues from $\mathscr{E}_{100}$-$\mathscr{E}_{150}$.

For the rotating billiard problem, the trajectory $x(t)$ is given in terms of its polar position (r, θ) from the centre of the circle, and the speed v and direction ψ of its motion. Conservation of energy restricts the trajectory to three dimensions; when $r = 1$ v is a function of θ:

$$v^2(\theta) = 2(\cos\theta + K - 1). \tag{4.1}$$

At each bounce $r = 1$, so the length ds of δx is given by

$$ds^2 = \left(1 + \frac{\sin^2\theta}{v^2}\right) d\theta^2 + v^2\, d\psi^2. \tag{4.2}$$

The Lyapunov exponent measures very clearly whether a trajectory belongs to a regular region or a chaotic one, and how chaotic that region is. If the limiting value

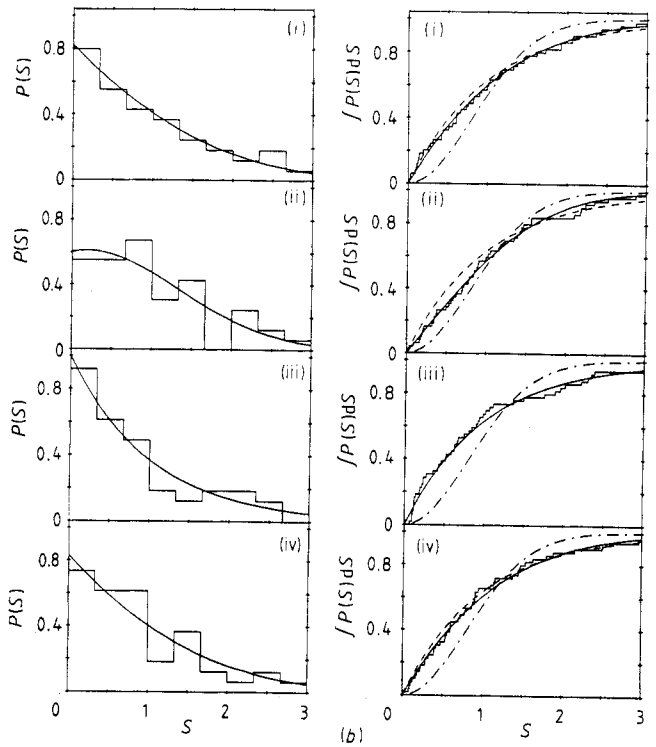

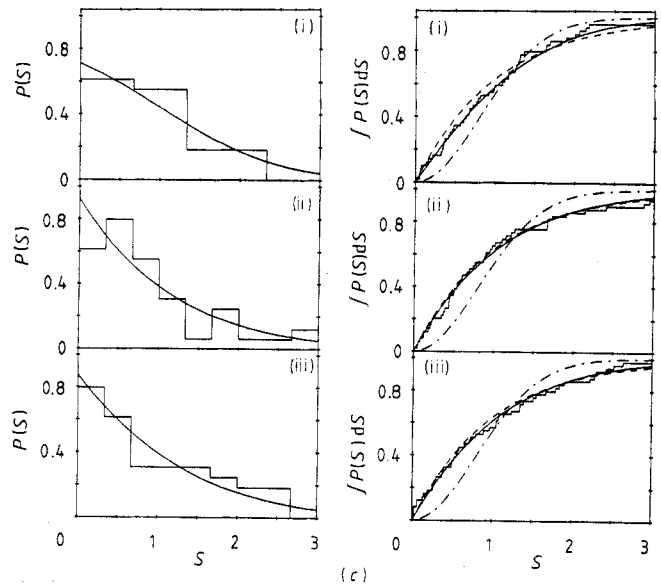

Figure 2. (continued)

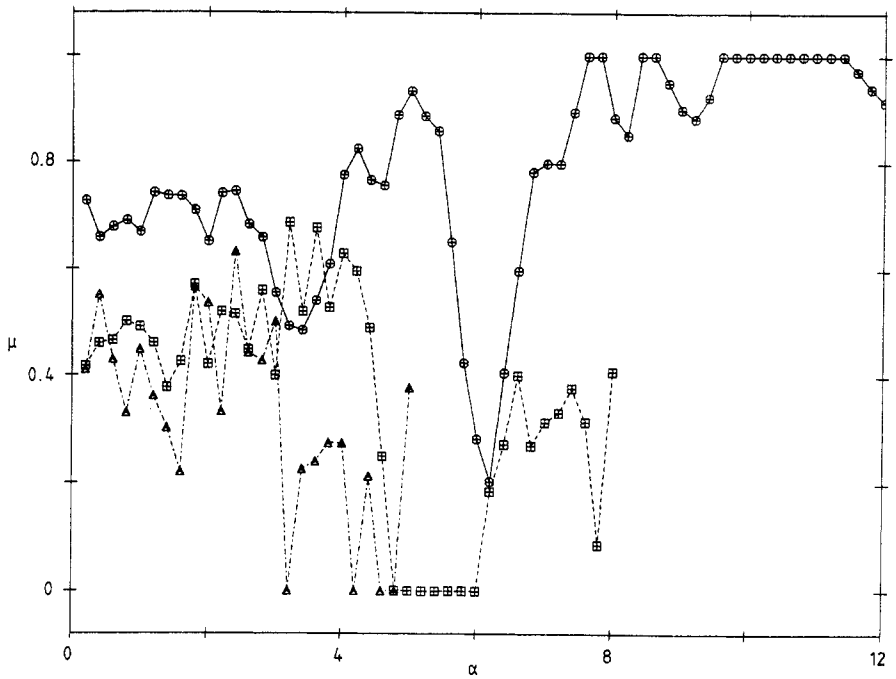

Figure 3. The EDF are fitted to a theoretical distribution of a uniform mixture of Poisson and Wigner energy levels. The resulting fitting parameter μ which measures the proportion of Wigner energy levels is plotted against $\alpha = 1/\hbar$. Note that $\mu = 1$ gives a pure Wigner distribution and $\mu = 0$ gives a pure Poisson distribution. The full curve is for the first 50 eigenvalues, the broken curve for the next 50, and the chain curve for $\mathscr{E}_{100}$-$\mathscr{E}_{150}$.

is zero (numerically set to some cutoff point) then the region is regular, otherwise it is chaotic. Negative values of Λ are never found for Hamiltonian systems because the sum of the characteristic exponents is always zero, so the maximal exponent is always positive.

The chaotic volume $\chi(K)$ is defined as the proportion of classically accessible phase space M which is chaotic; mathematically

$$\chi(K) = \frac{\int_M \Theta(\Lambda(\theta, \psi))\, \mathrm{d}\mu}{\int_M \mathrm{d}\mu} \tag{4.3}$$

where μ is the Liouville measure of the flow, and using equation (4.2) we find

$$\mathrm{d}\mu = (v^2 + \sin^2\theta)^{1/2}\, \mathrm{d}\theta\, \mathrm{d}\psi. \tag{4.4}$$

To calculate χ, a Monte Carlo method is used. A uniform distribution of random points in (θ, ψ) space is chosen. The Lyapunov exponent is calculated for each trajectory starting at these points, and if $\Lambda > 0.05$ it is accepted as chaotic. The Monte Carlo estimate is

$$\int_M f(\theta, \psi)\, \mathrm{d}\theta\, \mathrm{d}\psi \simeq \mathrm{Vol}(M)\left(\langle f\rangle \pm \sqrt{\frac{\langle f^2\rangle - \langle f\rangle^2}{N}}\right) \tag{4.5}$$

where N is the number of Lyapunov exponents sampled, and $\langle f\rangle$ denotes the mean

value of f. The numerator of (4.3) is calculated using this. The denominator was found by the same method, and it was also calculated by a quadrature method in order to test the Monte Carlo method for accuracy.

For each energy K, Lyapunov exponents for 250 points were calculated for 300 bounces. The resulting graph is plotted in figure 4. The statistical error from the Monte Carlo integration is much larger than the systematic error due to evaluating $\Lambda(x)$ for this number of bounces, so the error bars are two standard deviations thick as evaluated by the Monte Carlo method. To compare this with the energy ranges used for level

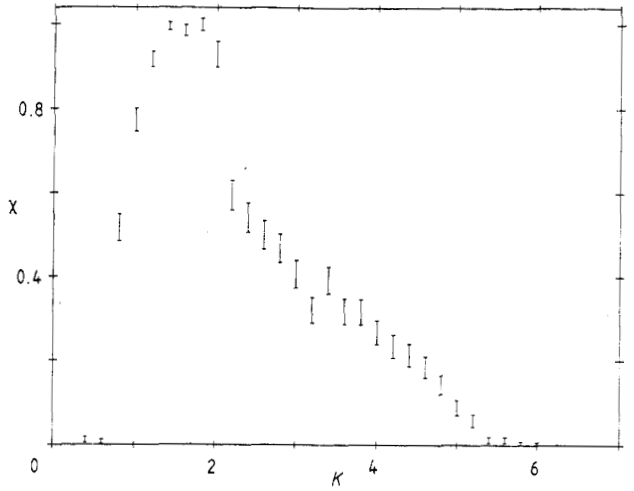

Figure 4. The chaotic volume χ of the rotating circular billiard against the energy K of the system.

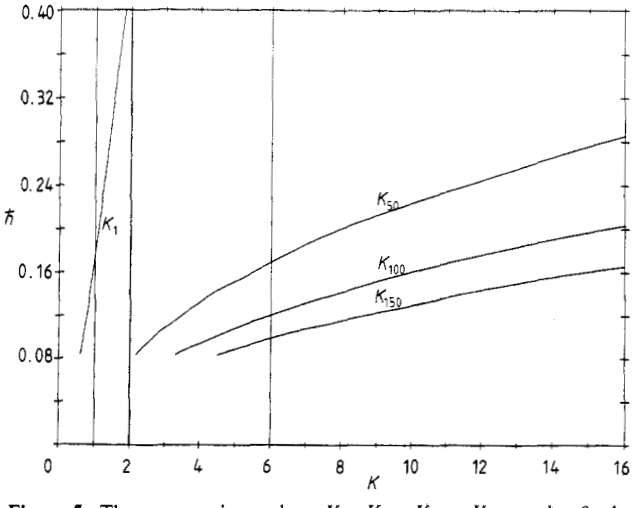

Figure 5. The energy eigenvalues K_1, K_{50}, K_{100}, K_{150} as $\hbar \to 0$, showing the convergence near $\hbar = \frac{1}{12}$ onto the most classically chaotic energy band. The thick vertical line shows the energy where $\chi(K)$ peaks and the classical motion is ergodic, and the thin lines on either side define the band of energies where $\chi > \varepsilon$ (for small ε) and where at least some of the motion is chaotic.

spacing distributions, figure 5 shows the relevant K_i eigenvalues plotted against $\hbar$, and the range of K for which the system is classically chaotic.

5. Discussion

In this paper we have attempted to explore the quantum mechanics of a simple system, which is classically chaotic in some regions of phase space. We have encountered numerical problems which restrict how far we can calculate the semiclassical limit. As $\hbar \to 0$, an impractically large matrix needs to be diagonalised in order to determine sufficient eigenvalues for a meaningful level-spacing distribution. This is to be expected; as the semiclassical limit is approached, less of the classical complexity of chaotic orbits is smoothed by quantum effects, and so higher-frequency terms become important.

This system has another problem which limits the applicability of the theory when $\hbar$ is large. The chaotic volume changes with energy, so to calculate $P(S)$ corresponding to a particular mixture of chaotic and regular orbits the energy interval must be small, otherwise the spectral statistics are not uniform. But for large $\hbar$, which includes most of the range of α that can be examined, the energy interval containing sufficient eigenvalues is too large.

These two difficulties mean that many of our results, particularly those made for very small α, are not expected to be in very good agreement with theoretical predictions. For large α we do expect our results to match with theory and indeed our results for $\alpha >= 9.4$ ($\hbar <= 1/9.4$) indicate that $P(S)$ is approaching a Wigner distribution for eigenvalues which are in a classically highly chaotic region. But we also have very unexpected behaviour in the transition region near $\alpha = 6$. The distribution $P(S)$ becomes very Poissonian, much more than would even be expected statistically (for such a small sample as 50 eigenvalues the distribution is not expected to fit the exact distribution particularly well) and this happens for eigenvalues that are in an energy range that spans the most classically chaotic energies of the system. The W^2 statistic for the Poisson distribution is 0.082 for $\alpha = 5.8$, and also low for nearby values of α. These are well within the significance level of 5%, $W^2_{cr} = 0.460$. We were not expecting good agreement with theory here; however neither were we expecting the system to appear as regular as this. Note also that the distribution is also very Poissonian near $\alpha = 6$ for the next two energy ranges (although the highest eigenvalues above the 100th are not as reliable as the lower ones for large α).

It is even more interesting when one compares this behaviour with that of the system when $\hbar$ is large ($\alpha < 1$), or when the circle is stationary (equivalent to $\alpha = 0$). Here, as expected, the system does not show very good Poisson behaviour, because the lowest 50 eigenvalues are not typical and it is the higher ones which behave as such. So even the most regular system anyone can think of, namely that of a perfectly circular billiard, does not appear to have as good Poisson statistics for low eigenvalues as our system when α is close to 6!

Many of the problems we have encountered were predicted by Berry [15]. Other work has been carried out on systems which show mixed regular and chaotic motion. Seligman *et al* have calculated level-spacing statistics and spectral rigidity for two particles in polynomial interactive and external potentials [17]. They have been able to calculate for smaller $\hbar$ and for much larger matrices, so their results show much better agreement with the semiclassical theory than ours. Matsushita and Terasaka

[18] and Scott [19] have also calculated level spacing statistics for mixing systems. But they have not found the effect mentioned above, nor have they calculated statistics for such large $\hbar$.

In conclusion, we found that our system behaves as expected in the semiclassical limit, according to random-matrix theory and theory relating classical chaotic phenomena to the semiclassical behaviour. But in the full quantum mechanical regime, there seems to be behaviour which is related to the above, but which present theory does not explain, and has not yet been developed. We see this as a challenge in the development of the theory of non-integrable quantum mechanics, although we have seen only a glimpse of the actual effect due to numerical limitations.

Acknowledgments

I would like to thank Drs D B Fairlie, R C Johnson and E F Corrigan for many useful discussions, and Drs A H Sehault and P J Green for help with the statistical analysis. This work was supported by a studentship from the SERC.

References

[1] Bunimovich L A 1979 *Commun. Math. Phys.* **65** 295-310
[2] Sinai Y G 1970 *Russ. Math. Surv.* **25** 137
[3] Robnik M 1984 *J. Phys. A: Math. Gen.* **17** 1049-74
[4] Robnik M and Berry M V 1985 *J. Phys. A: Math. Gen.* **18** 1361-78
[5] Berry M V and Robnik M 1986 *J. Phys. A: Math. Gen.* **19** 649-68
Robnik M and Berry M V 1986 *J. Phys. A: Math. Gen.* **19** 669-82
[6] Fairlie D B and Siegwart D K 1988 *J. Phys. A: Math. Gen.* **21** 1157-65
[7] Porter C E (ed) 1965 *Statistical Theories of Spectra: Fluctuations* (New York: Academic)
[8] Berry M V and Tabor M 1977 *Proc. R. Soc.* A **356** 375
[9] Bohigas O and Giannoni M J 1984 *Mathematical and Computational Methods in Nuclear Physics* (*Lecture Notes in Physics* **209**) ed J S Dehesa, J M Gomez and A Polls (Berlin: Springer) pp 1-99
[10] Seligman T H and Verbaarschot J J M 1985 *Phys. Lett.* **108A** 183-7
[11] Abramowitz M and Stegun I A 1965 *Handbook of Mathematical Functions* (New York: Dover)
[12] Press W H, Flannery B P, Teukolsky S A and Vetterling W T 1986 *Numerical Recipes* (Cambridge: Cambridge University Press)
[13] Berry M V 1983 *Chaotic Behaviour of Deterministic Systems, Les Houches Summer School Lectures XXXVI* ed R H G Helleman and G Joos (Amsterdam: North-Holland)
[14] Kotz S, Johnson N L and Read C B (eds) 1982 *Encyclopedia of Statistical Sciences* vol 2 (New York: Wiley) pp 451-4
[15] Berry M V and Robnik M 1984 *J. Phys. A: Math. Gen.* **17** 2413-21
[16] Bennettin G and Strelcyn J M 1978 *Phys. Rev.* A **17** 773
[17] Seligman T H, Verbaarschot J J M and Zirnbauer M R 1985 *J. Phys. A: Math. Gen.* **18** 2751-70
[18] Matsushita T and Terasaka T 1984 *Chem. Phys. Lett.* **105** 511
[19] Scott A C Private communication